

**TITLE:** CORRELATION OF THE GROWTH OF CHINESE HAMSTER V<sub>2</sub>79-171b  
MULTICELLULAR SPHEROIDS WITH CYTOKINETIC PARAMETERS

**AUTHOR(S):** T. S. Johnson, LS-1  
E. Bain, LS-1  
M. R. Raju, LS-1  
J. C. Martin, LS-2

**MASTER**

**SUBMITTED TO:** The Seventh Engineering Foundation Conference  
on Automated Cytology to be published in their  
Proceedings

DISCLAIMER

By acceptance of this article, the publisher recognizes that the U.S. Government retains a nonexclusive, royalty-free license to publish or reproduce the published form of this contribution, or to allow others to do so, for U.S. Government purposes.

The Los Alamos Scientific Laboratory requests that the publisher identify this article as work performed under the auspices of the U.S. Department of Energy.

University of California



**LOS ALAMOS SCIENTIFIC LABORATORY**

Post Office Box 1683 Los Alamos, New Mexico 87545

An Affirmative Action/Equal Opportunity Employer

## Multicellular Spheroid Volume and Cytokinetics

.

Correlation of the Growth of Chinese Hamster V<sub>2</sub>79-171b  
Multicellular Spheroids with Cytokinetic Parameters\*†

T. S. Johnson<sup>1</sup>, E. Bain<sup>1</sup>, M. R. Raju<sup>1</sup>, and J. C. Martin<sup>2</sup>

<sup>1</sup>Toxicology Group, LS-1  
<sup>2</sup>Biophysics Group, LS-2  
Life Sciences Division  
University of California  
Los Alamos Scientific Laboratory  
Los Alamos, New Mexico 87545 USA

Mailing address for proofs: T. S. Johnson  
Toxicology Group, LS-1, MS 880  
Los Alamos Scientific Laboratory  
P. O. Box 1663  
Los Alamos, New Mexico 87545

\*This paper was presented at the Seventh Engineering Foundation Conference  
on Automated Cytology, 25-30 November 1979.

†This work was performed under the auspices of the U. S. Department of  
Energy, with joint support from Grant No. 22585-01 from the National Cancer  
Institute, Department of Health, Education, and Welfare.

## SUMMARY

The volumes of Chinese hamster V<sub>2</sub>79-171b multicellular spheroids grown in spinner culture were measured and correlated to DNA distribution and cell volume distribution information. Spheroid growth curves were obtained over a 21 day period using both electronic cell volume measurements and microscope micrometer sizing. The spheroids were collected from the aperture tube after electronic sizing, and single cell suspensions were prepared via trypsinization. Saline-washed cells were then stained with mithramycin and analyzed as unfixed or ethanol-fixed cells for both cell volume and DNA fluorescence measurements. Spheroid growth was determined to have an initial 3 to 9 day rapid growth phase, and a slow phase from 10 to 21 days. The single cell volume distributions of cells obtained from spheroids were dependent on spheroid volume and the relative proportions of small volume noncycling cells to large volume cycling cells comprising the spheroids were also dependent on spheroid volume. DNA distribution data and dual parameter DNA distribution cell volume contour patterns obtained for single cells dissociated from spheroids were closely related to the measured spheroid volume and revealed that the fraction of small, hypoxic G<sub>0</sub>-like cells was greatest in old, large spheroids.

Indexing Terms: Spheroids, Cytokinetic, Flow Cytometry, DNA Distributions, and Cell Volume.

## INTRODUCTION

Tumor growth and delay measurements as well as cell-cycle measurements have been widely used as tumor biology endpoints (22,24,8). A better understanding of tumor kinetics might result from detailed correlative information for tumor growth dynamics in relation to cell-cycle kinetic properties of subpopulations comprising the tumor.

Multicellular spheroids are of intermediate complexity, between in vitro monolayer cultured cells and subclinical size in vivo nodular tumors or early metastatic foci. Spheroids are comprised of heterogeneous subpopulations (6,7) and provide a useful cell system for studying growth dynamics by electronic volume (2) (i.e., Coulter principle) and for monitoring the cytokinetic DNA distribution and cell volume distributions of cells which comprise the spheroids. To date, electronic cell volume, enumeration and sizing (2) of single mammalian cells have been extensively used and the underlying theory described (1,2,12,25,26). Conventional Coulter-type apertures having 10 to 2000  $\mu$  dia. orifices are available for single cell and large particle sizing (14). Various reports have described the usefulness of measuring cell volume in relation to cell-cycle information either separately (13,16,19,29) and in coincidence with other parameters (4,11,20,23,28).

In the present report, the growth of V<sub>2</sub>79-171b Chinese hamster lung multicellular spheroids were studied and correlated with flow cytometric measured cell-cycle DNA distributions and cell volume distributions for single cells comprising the spheroids. The purpose was: first, to use electronic volume of spheroids as an accurate measure of spheroid volume for describing spheroid growth curves; and second, to directly correlate

spheroid volume with the single cell DNA distributions and cell volume distributions for cells comprising the same spheroids.

## MATERIALS AND METHODS

### Growth of Multicellular Spheroids

Chinese hamster lung cells (V<sub>2</sub>79-171b) were grown as monolayer cultures using basal medium/Eagle (BME) plus 15% fetal calf serum (FCS). Spheroid cultures were prepared by seeding freshly trypsinized cells into BME plus 5% FCS at a concentration of  $1.5 \times 10^4$  cells/ml as previously described (7). Routinely, spheroid cultures were maintained for 21 days and aliquots of suspended spheroids were sampled at various times starting at day 0.

### Morphology and Microscopic Sizing of Spheroids

Freshly harvested V<sub>2</sub>79-171b spheroids were gently washed in 5°C physiological saline, and either supravital-stained for 5 min. with 0.1 mg/100 ml acridine-orange (Basic Orange 14, Matheson, Coleman, Bell, Norwood, Ohio), or with mithramycin (3). The morphology of freshly stained spheroids was examined by fluorescence microscopy, and size measurements were made using a calibrated eye-piece micrometer. These measurements were then compared statistically to the electronic volume measurements.

### Electronic (Coulter) Volume Measurements of Spheroids

Electronic volume measurements of intact multicellular spheroids were obtained from freshly harvested spheroids which had been cultured for varying periods ranging from 0 to 21 days. Spheroids suspended in saline, were hydrodynamically focused through an aperture (Coulter Electronics, Inc., Hialeah, Florida) with a 1000  $\mu$  dia. sapphire orifice. The focusing

tube consisted of a 7-cm long stainless steel tube (i.d. 2.6 mm) with a press-fit Rexolite plastic (Polymer Corp., Reading, Pennsylvania) 800  $\mu$  dia. orifice, mounted on an X, Y, Z micromanipulator (Fig. 1).

Signals arising from spheroids passing through the orifice were amplified using a standard LASL designed electronic amplifier circuit (28) as illustrated in Fig. 1. The amplitudes of the long analog signals (100 to 250  $\mu$  sec. rise times) were captured by a gated peak sense-and-hold circuit (28). Each signal amplitude was held some 50  $\mu$  sec. and a short portion of this held signal (approx. 10  $\mu$  sec. wide pulse) was gated out in order to provide a rectangular pulse shape and pulse duration that the analog to digital converter (ADC) would accommodate. Each pulse was then digitized by a Northern Scientific model 623 ADC. The digitized data were stored using a Northern Scientific model 636 pulse height analyzer (PHA) linked to a LSI-11/2 microprocessor (Digital Equipment Corporation (DEC), Maynard, Massachusetts), which features several peripheral devices including: graphics terminal; dual floppy disc; and hard copy. The software operating system was RT-11 version 3B (DEC).

#### Multiparameter Flow Cytometric Measurements of Single Cells

Spheroids were collected from the aperture tube immediately after sizing, and single cell suspensions prepared by trypsinization, followed by two saline washes at 5°C (10 min, 800 rpm centrifugation, each wash). The dissociated spheroid cells were subsequently analyzed as either unfixed cells stained for 5 min with mithramycin in saline or as ethanol fixed cells (2-3 hr fixation, followed by a saline wash prior to staining with mithramycin) using mithramycin concentrations similar to that previously described (3). These mithramycin-stained cells were then analyzed on the

Los Alamos Computer-Based Multiparameter Cell Sorter (17) with laser excitation at 457.9 nm. The flow cytometric data acquisition and display programs used have been reported (21). DNA distributions were determined by means of computer programs described previously (5,9).

## RESULTS

### Spheroid Morphology and DNA Fluorescence Staining Properties

Chinese hamster lung multicellular spheroids ( $V_{279-171b}$ ) growing in spinner culture for 0 to 21 days were studied using fluorescent microscopic examination of wet-mount preparations of unfixed spheroids stained with either acridine-orange or mithramycin. Detailed cytological and morphological characteristics were readily evident using 300 to 500 nm broad band excitation and a 530 nm barrier filter. A-O stained spheroids displayed differential green nuclear fluorescence and orange to red cytoplasmic fluorescence (Fig. 2). Interphase and mitotic phase cells were readily distinguishable upon examination by oil immersion microscopy. Mithramycin-stained spheroids showed comparable cytological detail, but were not used for micrometer sizing due to rapid fluorescence fading. Comparison of the mithramycin staining properties of  $V_{279-171b}$  cells indicated that the emission spectra were similar for unfixed and ethanol-fixed cells. More importantly, the DNA fluorescence per cell detectable by flow cytometry were comparable for unfixed and ethanol-fixed, saline washed cells. Therefore, essentially the same DNA distributions could be obtained with unfixed as with fixed cells (10). The main difference observed has been that the mithramycin-binding equilibrium time is longer for unfixed  $V_{279-171b}$  cells (approx. 3 to 4 min) than for ethanol-fixed saline washed cells (approx.  $\leq$  1 min) as described in separate studies (15).

## Spheroid Volume in Relation to DNA Distribution and Cell Volume Distribution

Spheroid electronic volume distributions were obtained at various times during the twenty-one day culture period using the instrument shown in Fig. 1. Figure 3 provides an example of the long analog pulses detected (100 to 250  $\mu$  sec. rise times) for spheroids together with a volume distribution curve obtained for 14 day old spheroids (mean diameter from micrometer measurement of  $\approx 512 \mu$ ). Immediately after each spheroid sample volume measurement, sedimented spheroids were collected from the aperture tube and dissociated into single cells via trypsinization for flow cytometric analysis. The results for spheroid volume measurements together with the DNA distributions obtained for the single cells from these same spheroids are shown in Fig. 4. The data of Fig. 4 represent one of two replicate experiments (7 sample periods per experiment with triplicate samples for each period) with the same results. The spheroid volume curve (dashed line, Fig. 4) describes Gompertzian growth dynamics (18), with a rapid growth phase the first 8 to 9 days followed by a slow growth phase from 10 to 21 days. Statistical comparison of the micrometer and electronic spheroid volume estimates indicated reasonable agreement ( $p = 0.05$ ).

The DNA distributions of spheroid cells were characterized by a rapid decrease in S and  $G_2M$  cells during the first 8 to 10 days followed by a relatively stable period from 10 to 21 days (Fig. 4).<sup>a</sup> Single cells transferred to spinner cultures on day 0 had DNA distributions of  $G_0/G_1 = 22$  to 23%, S = 63 to 65%, and  $G_2M = 10$  to 11%. By day 10, some 21-23% of the spheroid cells were in S-phase, about 65% in  $G_0/G_1$  and 9 to 10% in  $G_2M$ . There was little change from day 10 to day 21. The time-dependency for

spheroid DNA distribution changes in relation to cell volume distribution changes were evident in dual parameter contour and isometric displays obtained for each of the seven sample periods from day 0 to 21 (e.g. see Fig. 5). The decrease in the S and G<sub>2</sub>M cycling cells evident during the first 10 day culture period occurred concomitant with a build-up in the proportion of small volume cells having G<sub>0</sub>/G<sub>1</sub> DNA fluorescence (Fig. 5). Table 1 shows the estimated cycling fractions (i.e., G<sub>1</sub> + S + G<sub>2</sub> + M) for cells from spheroids having different volumes (i.e., times in culture). With time, the  $\frac{G_0 + G_1}{S + G_2 + M}$  ratio increased, particularly during the first 10 day culture period, e.g., from 0.32 at day 0 to 1.86 at day 11. This reflects the build-up of small volume, noncycling hypoxic and nutrient deficient G<sub>0</sub>-like cells in the spheroids, as does the ratio of estimated cycling fraction to spheroid volume (Table 1). For comparison, published mitotic indices and <sup>3</sup>H-TdR labeling indices data for the same spheroid line (7) are also shown in Table I.

---

<sup>a</sup>The cell dissociation method used (6,7) yielded consistent results which were considered to be representative of the intact spheroid population. Experiments are in progress to further test whether or not spheroid trypsinization yields single cell preparations having noncycling and cycling cells in total agreement with <sup>3</sup>H-thymidine and <sup>125</sup>I-iododeoxyuridine radiotracer kinetic and autoradiographic labeling data.

## DISCUSSION

The results demonstrate the use of electronic volume measurement for multicellular spheroids. Statistically accurate ( $p \leq 0.05$ ) volume measurements of Chinese hamster V<sub>2</sub>79-171b multicellular spheroids were obtained for growth descriptive analysis (e.g., see Fig. 3). Spheroid volume and growth dynamics were compared with DNA distribution and cell volume distribution data obtained from the cells which comprised the same spheroids. As the spheroids grew larger, there was a concomitant increase in the proportions of cells having small cell volume and G<sub>0</sub>/G<sub>1</sub> DNA fluorescence. This build-up of (presumably) noncycling cells was shown to be related to a decreased spheroid growth rate based on the spheroid electronic volume measurements (see Fig. 4 and Table 1). By utilizing DNA distribution data together with a few reasonable assumptions (footnotes of Table 1), the cycling cell fractions for spheroids of different volumes were estimated. For example, cycling fraction values of 0.99 and 0.41 were obtained for V<sub>2</sub>79-171b spheroids sampled at 0 and 18 days in culture respectively (Table 1). Our cycling fraction estimates were in good agreement with previously published mitotic indices and <sup>3</sup>H-TdR labeling data for the same spheroid line (7).

Achievement of accurate resistance-charge pulse amplitude sensing as in the present study (or pulse-shape measurements) for spheroids depends on several basic factors. Unlike single cells, spheroids tend to settle-out of suspension; hence stirring and hydrodynamic focusing are required. We used electrolyte flow through the sensing aperture to focus the spheroids emerging from a focusing tube. Hydrodynamic focusing was utilized to minimize edge effects in the electric field and was similar in nature to

the approach described by Spielman and Goren, 1968 (27) for analyzing plastic microspheres. Since spheroids grow to large volumes (e.g.,  $5 \times 10^7 \mu^3$ ), the volume-to-orifice diameter is more critical when measuring spheroids than when sizing single cells (12,25,26). A 1000  $\mu$  dia. orifice was used in this study, but we plan to employ a 2000  $\mu$  sapphire orifice with additional sheath flow in future studies to improve signal quality. To accommodate the unusually long analog pulses of up to 250  $\mu$  sec. rise time, a gated peak sense-and-hold circuit compatible with the ADC was used. Direct correlation of spheroid volume information with flow cytometric parameters requires analysis of single cells. This was accomplished by gently "trapping" spheroids after electronic sizing by inserting a nylon mesh into the top of the aperture tube and pipetting the sedimented spheroids out of the tube at the end of each run. The harvested spheroids were then trypsinized into single cells, which were further analyzed for cell volume and DNA distribution information.

Spheroid volumes were estimated in the present study by gated pulse amplitude measurement, which is generally but not always independent of particle shape, orientation, and density (2,12,14). Comparison of the spheroid electronic volume data with volume estimates obtained from two-dimensional microscopic micrometer measurements indicated that the two different methods agreed at the  $p \leq 0.05$  statistical level. In terms of future developments, it would be worthwhile to use other techniques to obtain spheroid volume information, e.g., pulse-rise time, pulse-width and integrated pulse sensing from the electronic signals; or pulse-rise time, and time-of-flight measurements, using light scatter and fluorescence signals from a laser-based flow cytometer. Finally, this method has potential for assessing chemical or physical agent-induced alterations in

spheroid growth. In addition, it should be feasible to study the changes of spheroid subpopulations, (e.g., noncycling vs cycling cells in relation to spheroid growth state or response to therapy), with more definitive analytical confidence than possible with present-available techniques.

## REFERENCES

1. Anderson JL, Quinn JA: The relationship between particle size and signal in Coulter-type counters. *The Rev Sci Inst* 42: 1257-1258, 1971
2. Coulter WH: High speed automated blood cell counter and cell size analyzer. *Proc Natl El Conf* 12: 1034-1040, 1956
3. Crissman HA, Tobey RA: Cell cycle analysis in twenty minutes. *Science* 184: 1297-1298, 1974
4. Crissman HA, Orlicky DJ, Kissane RJ: Use of the two parameter (DNA and cell size) flow cytometric analysis for determining the effects of potential chemotherapeutic agents. *Acta Pathol et Microbiol Scand* (in press)
5. Dean PN, Jett JH: Mathematical analysis of DNA distributions derived from flow microfluorometry. *J Cell Biol* 60: 523-527, 1974
6. Durand RE, Sutherland RM: Dependence of the radiation response of an in vitro tumor model on cell cycle effects. *Cancer Res* 33: 213-219, 1973
7. Durand RE: Cell cycle kinetics in an in vitro tumor model. *Cell & Tissue Kinet* 9: 403-412, 1976
8. Hermans AF, Barendsen GW: The importance of proliferation kinetics and clonogenicity of tumor cells for volume responses of experimental tumors after irradiation. In: *Radiation Research-Biomedical, Chemical, and Physical Perspectives*. Academic Press, New York, 1975, p. 834-849
9. Jett JH: Mathematical analysis of DNA histograms from asynchronous and synchronous cell populations. In: *Proceedings 3rd International Symposium on Pulse-Cytophotometry*, Lutz D (ed). European press, Ghent, Belgium, 1978, p. 93-102
10. Johnson TS, Tokita N, Bain E, Raju MR: In vitro V79-171b Multi-cellular spheroid cytokinetic and cell-survival response to single vs fractionated x-irradiation. In: *Annual Report of the Biomedical and Environmental Research Program of the LASL Health Division, Jan-Dec, 1978*, p. 129-132
11. Kachel V, Glossner E, Kordwig E, Ruhenstroth-Bauer G: FLUVO-Metricel, a combined cell volume and cell fluorescence analyzer. *J Histochem Cytochem* 25: 804-812, 1977
12. Kachel V: Electrical resistance pulse sizing (Coulter sizing). In: *Flow Cytometry and Sorting*, Melamed MR, Mullaney PF, Mendelsohn ML (eds). John Wiley & Sons, New York, 1979, p. 61-104

13. Kal HB: Distributions of cell volume and DNA content of Rhabdomyosarcoma cells growing in vitro and in vivo after irradiation. Europ J Cancer 9: 77-79, 1973
14. Kingman S: Particle characterization. In: Systems Materials Analysis Vol. IV, Richardson JH, Peterson RV (eds). Academic Press, New York, 1978, p. 194-196
15. Martin JC, Swartzendruber DE, Travis GL, Johnson TS: A new method for kinetic measurement in flow cytometry. Analyt and Quantit Cytometry (in preparation)
16. Meistrich ML, Grdina DJ, Meyn RE, Barlogie B: Separation of cells from mouse solid tumors by centrifugal elutriation. Cancer Res 37: 4291-4296, 1977
17. Mullaney PF, Steinkamp JA, Crissman HA, Cram LS, Holm DM: Laser flow microphotometers for rapid analysis and sorting of individual mammalian cells. In: Laser Applications in Medicine and Biology, Wolbarsht ML (ed). Plenum Press, New York, 1974, p. 151-204
18. Norton L, Simon R: Growth curve of an experimental solid tumor following radiotherapy. J Natl Cancer Inst 58: 1735-1741, 1977
19. Petersen DF, Anderson EC, Tobey RA: Mitotic cells as a source of synchronized cultures. In: Methods in cell physiology, Vol. 3. Academic Press, New York, 1968, p. 347-370
20. Raju MR, Johnson TS, Tokita N, Gillette EL: Flow cytometric applications of tumor biology: Prospects and pitfalls. Brit J Radiol 41: Suppl IV (March 1980)
21. Salzman GC, Hiebert RD, Crowell JM: Data acquisition and display for a high-speed cell sorter. Comput and Biomed Res 11: 77-88, 1978
22. Schabel FM Jr: The use of tumor growth kinetics in planning "curative" chemotherapy of advanced solid tumors. Cancer Res 29: 2384-2389, 1969
23. Shackney SE: Interrelationships among the DNA content distribution, cell kinetics, and cell morphology: Theoretical considerations, experimental correlations, and clinical implications. In: Growth kinetics and Biochemical Regulation of Normal and Malignant Cells. The Williams & Wilkins Co., Baltimore, 1977, p. 391-409
24. Simpson-Herren L: Kinetics and tumor models. Cancer Chemoth Rep 5: 83-88, 1975
25. Smythe WR: Flow around a sphere in a circular tube. The Phys of Fluids 4: 756-759, 1961
26. Smythe WR: Flow around spheroids in a circular tube. Phys Fluids 7: 633-638, 1964

27. Spielman L, Goren SL: Improving resolution in Coulter counting by hydrodynamic focusing. J. Colloid & Interface Sci 26: 175-182, 1968
28. Steinkamp JA, Fulwyler MJ, Coulter JR, Hiebert RD, Horney JL, Mullaney PF: A new multiparameter separator for microscopic particles and biological cells. Rev Sci Instrum 44: 1301-1310, 1973
29. Valet G, Fischer B, Sundergeld A, Hanser G, Kachel V, Ruhenstroth-Bauer G: Simultaneous flow cytometric DNA and volume measurements of bone marrow cells as sensitive indicator of abnormal proliferation patterns in rat leukemias. J Histochem Cytochem 27: 398-403, 1979

Table 1. Estimated cycling fraction<sup>S</sup> for V<sub>2</sub>79-171b spheroids based on flow cytometric DNA fluorescence data. Previously published mitotic indices and <sup>3</sup>H-Thymidine(<sup>3</sup>H-TdR) autoradiographic labeling data(Durand, 1976, ref. 6) are also shown for comparison.

Time in Culture (days)	Flow Cytometric Measurements		Durand(1976)	
	$\frac{G_0 + G_1}{S + G_2M}$	Estimated <sup>b</sup> Cycling Fract.	Estimated Cycling Fract. (M.I.)	( <sup>3</sup> H-TdR)
0	0.32	0.99	1.05	0.99
1	0.45	0.88-0.90	0.93	0.93
3	0.79	0.71-0.72	0.75	0.72
6	1.22	0.59-0.60	0.66	0.62
11	1.86	0.45-0.46	0.46	0.55
18	2.22	0.39-0.40	0.40	0.44
21	2.33	0.38-0.39	---	---

<sup>b</sup> Assumptions:

1.  $G_0 = 0.01$  at  $t=0$  day (6).

2. Rate of cell-cycle traverse constant at  $t=0$  to 21 days (6).

3. The fraction of cells in  $G_1$  increases and decreases proportionally with the fraction of cells in S plus  $G_2M$  phases, where

$$G_1(t) = \frac{G_1(t_0)}{S(t_0) + G_2M(t_0)} \times S(t) + G_2M(t)$$

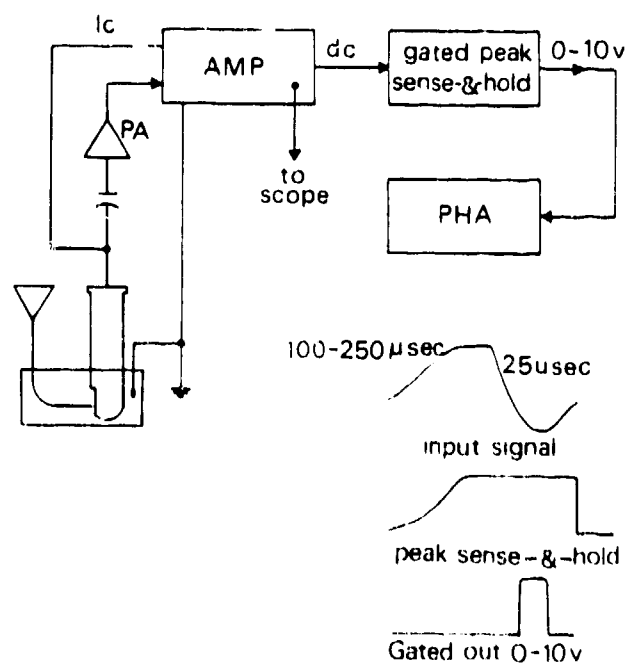
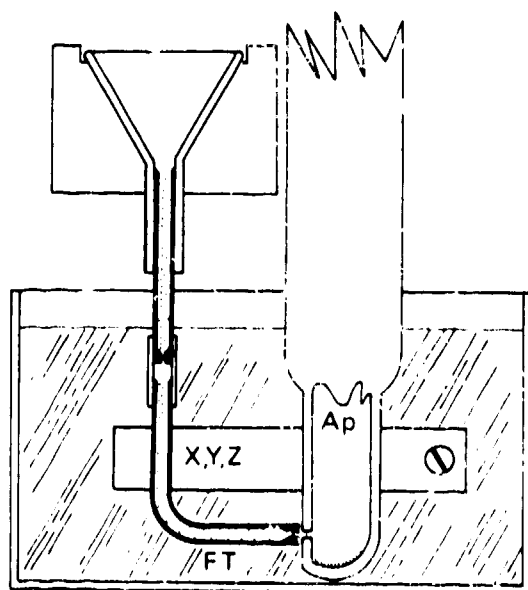
Fig. 1. Electronic volume measurements of multicellular spheroids. (A) Diagrammatic illustration of the Coulter aperture (Ap) and hydrodynamic focusing tube, (FT) and micromanipulator (X,Y,Z), with spheroids passing through the 1000  $\mu$  orifice and collecting at the bottom of the aperture tube. (B) block diagram of the electronic volume circuitry. The long analog pulses were processed by a gated peak-sense and hold circuit, then digitized for pulse-height analysis.

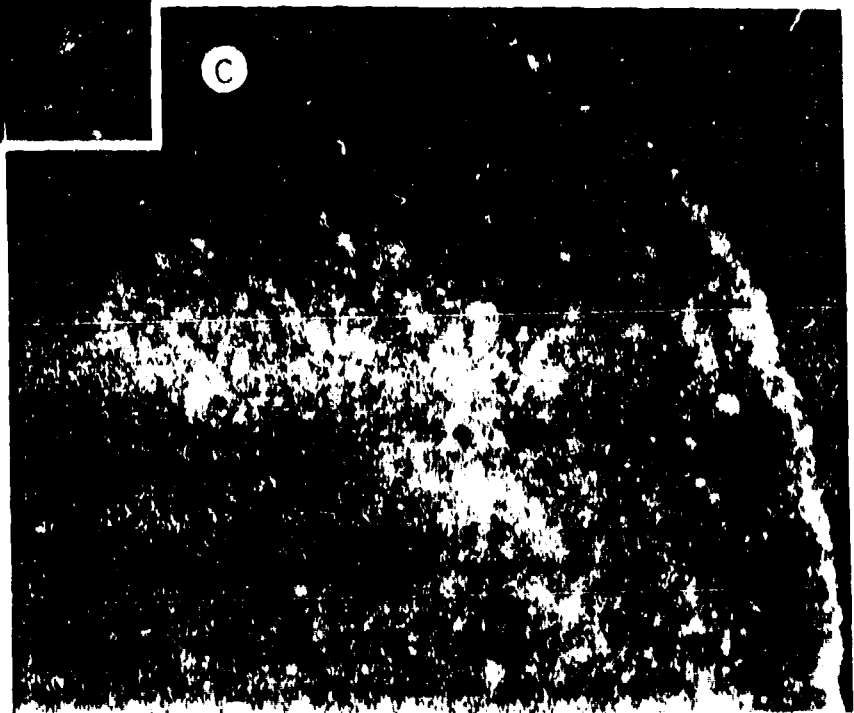
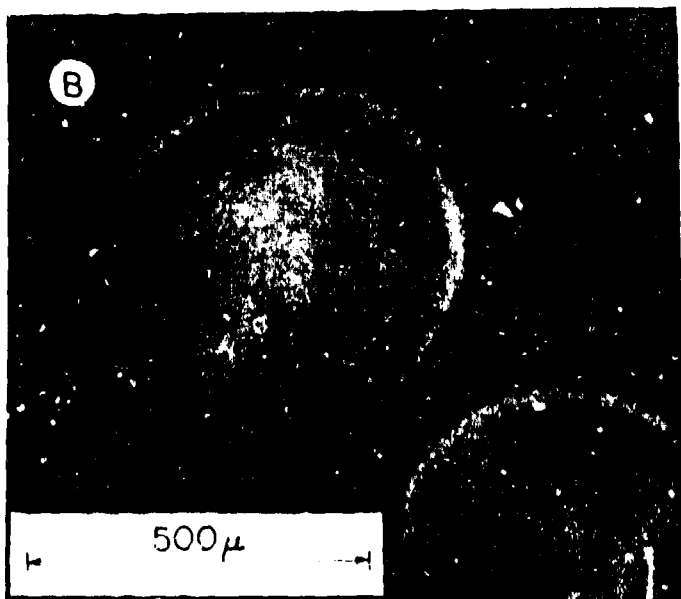
Fig. 2. Photomicrographs of fluorescent, acridine-orange stained V<sub>2</sub>79-171b Chinese hamster lung multicellular spheroids. (A) Single cells obtained via trypsinization from the spheroids shown in B and C. (B) Low power view of 14 day cultured spheroids. (C) Higher power view of one of the spheroids, showing cells in the outer region.

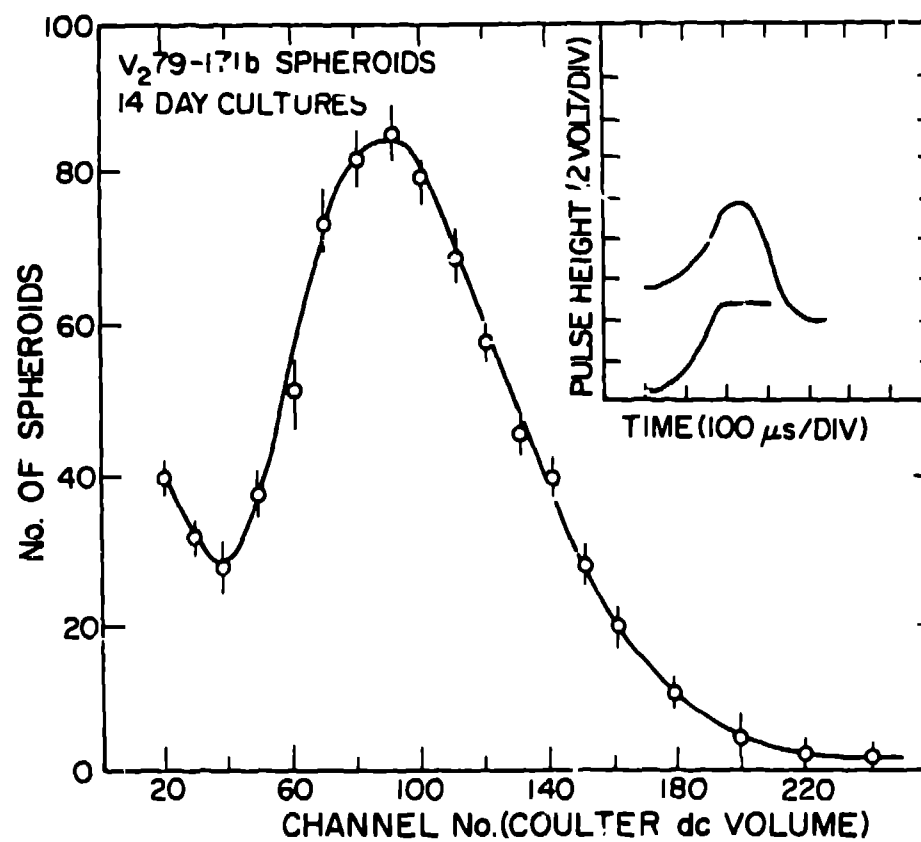
Fig. 3. Coulter volume distribution of V<sub>2</sub>79-171b Chinese hamster lung multicellular spheroids cultured for 14 days. The error limits shown (o) represent statistical standard deviations. Insert (upper trace) an oscilloscope trace of a spheroid Coulter volume pulse (approx. 250  $\mu$  sec. rise time) and (lower trace) the corresponding gated peak sense-and-hold pulse.

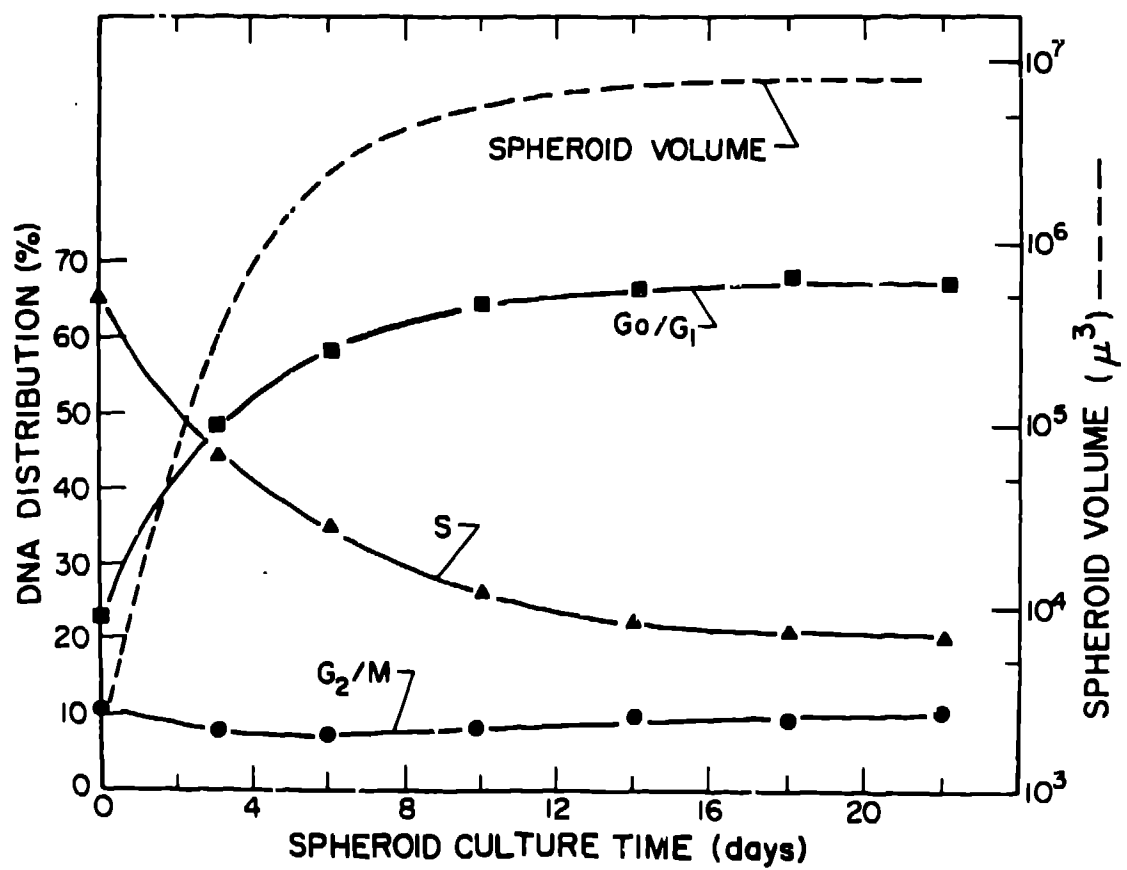
Fig. 4. Time-dependency curves for V<sub>2</sub>79-171b Chinese hamster lung multicellular spheroid electronic volume and DNA distributions for cells dissociated from the same spheroids. Dashed lines (---) represent the Gompertzian spheroid growth curve obtained by plotting the electronic volumes of spheroids cultured from 0 to 21 days. Solid lines (—) show representative mithramycin flow cytometric DNA distribution data obtained for single cells dissociated from these spheroids.

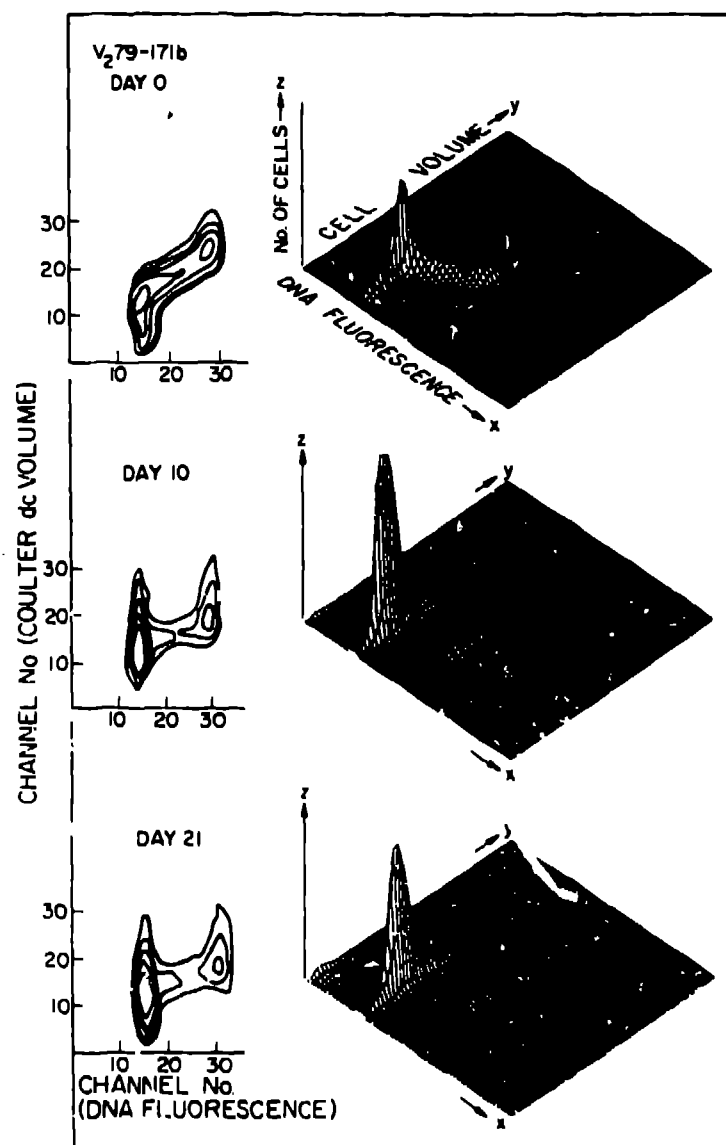
Fig. 5. Time-dependency for the DNA distributions and electronic cell volume distributions of single cells obtained from V<sub>2</sub>79-171b Chinese hamster lung multicellular spheroids. The dual parameter DNA fluorescence/electronic cell volume data are plotted for 50,000 unfixed, mithramycin-stained cells, obtained from spheroids sampled at 0, 10, and 21 days in culture. (Left) contours are plotted at elevations of 25, 50, 100, 200 and 500 cells. (Right) isometric plots of the same data.











15-7-77